Quadrupolar projection of excluded-volume interactions in biaxial nematic liquid crystals

Riccardo Rosso and Epifanio G. Virga
Dipartimento di Matematica and CNISM, Università di Pavia, via Ferrata 1, 27100 Pavia, Italy
(Received 10 March 2006; revised manuscript received 14 July 2006; published 29 August 2006)

We compute the quadrupolar approximation to the excluded-volume interaction between hard spherocuboids, which applies to both platelets and spheroplatelets as special cases. We show that this approximation can be written as the superposition of two London interactions: one attractive and the other repulsive. This conclusion also proves why the phase diagram for the excluded-volume interaction of spherocuboids is expected to feature a direct isotropic-to-biaxial transition at a single Landau point.

DOI: 10.1103/PhysRevE.74.021712 PACS number(s): 61.30.Cz

I. INTRODUCTION

Statistical theories of uniaxial liquid crystals span between two extreme approaches. The first approach goes back to Onsager's paper [1], where the ordering isotropic-to-nematic transition was found by assuming that nematogenic molecules can be represented as elongated hard cylinders only interacting by excluded volume. The second approach is Maier and Saupe's mean-field description of thermotropic liquid crystals [2]. These theories differ in an essential respect. Onsager's is fully entropic, whereas Maier and Saupe's is not. This entails other differences. Onsager's model is athermal with the number density acting as a control parameter, whereas in Maier and Saupe's theory the temperature is the control parameter. Moreover, while Onsager's approach focuses on anisotropic, short-range, repulsive interactions, Maier and Saupe's treatment is entirely formulated in terms of anisotropic long-range, attractive interactions [3]. Despite these differences, the two approaches have a common formal structure [4] that can be used to map, to some extent, one model into the other [5]. Both theories involve drastic simplifications and they become exact in asymptotic cases: Onsager theory is exact in the limit of infinitely long molecules at extremely low concentrations, while Maier and Saupe theory is exact only when the molecular interactions are infinitely long-range.

Although the hard-core model of Onsager gave rather poor predictions for the isotropic-to-nematic transition, further developments in the statistical mechanics of simple fluids suggest that anisotropic hard-body interactions need to be understood before theories of softer interactions become predictive [6]. Precisely, the perturbation theory of Weeks, Chandler, and Andersen [7] showed that the repulsive component of the intermolecular forces determines the structure of simple fluids at equilibrium, while the attractive component could be treated as a perturbation. Hard-core interactions become then important as a means to mimic the repulsive component of the intermolecular potential.

In the original papers of both Onsager and Maier and Saupe, nematic molecules were treated as *uniaxial*, that is, endowed with $D_{\infty h}$ symmetry around their long axis. More realistic models represent these molecules as *biaxial*, with three orthogonal axes of symmetry: in the crystallographic group language, biaxial molecules exhibit a D_{2h} symmetry. A model *à la* Maier-Saupe for biaxial molecules was proposed long ago by Straley [8]. This model builds a mean-field theory upon the most general quadrupolar effective interaction Hamiltonian H compatible with the D_{2h} symmetry. Such a generality, however, was lost in a specific choice for the coefficients in H, made to reproduce the excluded-volume interaction between platelets at given relative orientations. The phase diagram obtained for a fixed choice of length-to-width ratio of the platelets showed a direct isotropic-to-biaxial transition at an isolated Landau point, where three phases, isotropic, nematic, and biaxial, coexist at equilibrium. Since then, this phase diagram had become typical for biaxial liquid crystals, also because it was found in mean-field theories starting from different intermolecular potentials, like quadrupolar approximations to anisotropic dispersion forces [9] or hard-core interactions between equal spheroplatelets [10]. It was only recently realized [11] that Straley's original quadrupolar potential could lead to a different phase diagram, also exhibiting a tricritical point in the uniaxial-to-biaxial transition line and a direct isotropic-to-biaxial transition. This eventually resulted to be the most general picture as it includes the one with a single Landau point as a special case [12].

It was shown in [12] that Straley's Hamiltonian H can always be decomposed in the sum of two diagonal, quadratic terms: when these terms are both attractive, we say that H is *fully attractive*, when one term is attractive and the other repulsive, while H is globally attractive, we say that H is *partly repulsive*. This paper explores the possibility that biaxial hard particles with a shape other than Straley's platelets, by only interacting through excluded volume, may embody partly repulsive quadrupolar interactions. Clearly, we do not expect such an interaction to be fully quadrupolar, but its quadrupolar projection, that is, its component in an appropriate finite-dimensional space is bound to be so. We move from the intuition that excluded-volume interactions are repulsive by their very nature.

In hard-core interactions, the excluded volume between two molecules is proportional to the second virial coefficient in the functional expansion of the configurational free energy. That is why many efforts have been made to find the excluded volume for bodies with biaxial symmetry, extending Onsager's calculations for elongated, uniaxial rods [1]. Two technical approaches have been followed to achieve this. The former relies on convex-body coordinate systems [13] and takes biaxial ellipsoids as prototypes for biaxial molecules. This is an approach with a long history and its

origins go back to Isihara [14] who explicitly computed the excluded volume between ellipsoids of revolution. The excluded volume between biaxial ellipsoids was first computed by Tijpto-Margo and Evans [15], and then recast in a different form [13]. In a second approach, biaxial bodies are obtained by *Minkowski addition* (see Chap. 2 of [16]) of a sphere and another, suitably chosen body. Mulder [17] first applied this technique to compute the excluded volume between two identical *spheroplatelets* and his results were generalized by Taylor [18] to the case of unequal spheroplatelets. Recently, Mulder [19] computed the excluded volume for an important class of convex bodies, the *spherozonotopes*. A *zonotope* is obtained by Minkowski addition of a certain number of segments. A spherozonotope is obtained by Minkowski addition of a zonotope and a sphere. By expressing the excluded volume between two convex bodies as the volume of an auxiliary body, and applying Steiner's formula, Mulder [19] computed the excluded volume between two arbitrary spherozonotopes.

Here, we are interested in *spherocuboids*, the spherozonotopes with biaxial symmetry. Intuitively, spherocuboids are bodies obtained by moving the center of a sphere all along the sides of a parallelepiped. They are general enough to encompass platelets and spheroplatelets as special cases, depending on the choice of the geometric parameters. By applying Mulder's results, we compute the quadrupolar projection of the excluded volume between two spherocuboids and we show that it is partly repulsive.

The detailed layout of this paper is as follows. In Sec. II, mainly based on Mulder's [10] bifurcation analysis, we introduce the quadrupolar projection of an effective interaction kernel. In Sec. III after adapting Mulder's formula [19] for the excluded volume between spherozonotopes to the case of two equal spherocuboids, we compute the quadrupolar projection of the excluded-volume interaction between spherocuboids, which is the main object of the paper. In Sec. IV, this result is compared with the general quadrupolar theory for biaxial nematics [12], and the quadrupolar component of the excluded-volume interaction of spherocuboids is shown to be partly repulsive. In Sec. V we summarize the conclusions of our paper and comment on the prospects they offer for future work. The paper is closed by four Appendixes: three are computational and one is historical in nature. The latter shows how the classical excluded-volume interaction put forward by Onsager can be obtained in the formalism adopted in this paper.

II. QUADRUPOLAR PROJECTIONS

In this section, we recall the main steps of Mulder's analysis [10] to study bifurcations from the isotropic into a nematic phase, either uniaxial or biaxial. Following Onsager's [1] approach, the free energy f per particle is written by truncating a virial expansion [10,20] as

$$\beta f[\Psi] = \int \Psi(\Omega)\ln \Psi(\Omega)d\Omega + \frac{\eta}{2}\int\int \Psi(\Omega_1)\Psi(\Omega_2)\mathcal{K}(\Omega_1,\Omega_2)d\Omega_1 d\Omega_2 + \beta\tilde{f}(\eta), \tag{2.1}$$

where $\beta := 1/kT$, T is the absolute temperature and k is the Boltzmann constant. Moreover, Ψ is the one-particle orientational distribution function, Ω_i is the set of angular variables for the ith molecule, and η is a positive control parameter which vanishes when the molecules do not interact and grows larger as they are more strongly coupled. Finally, $\mathcal{K}(\Omega_1,\Omega_2)$ is the effective *anisotropic* interaction kernel. The first term on the right-hand side of Eq. (2.1) is an ideal gas contribution, while $\tilde{f}(\eta)$ is an isotropic correction that is independent of Ψ, and so will be disregarded in the sequel.

The function $\mathcal{K}$ obeys some general properties, like being a real function, invariant under a simultaneous rotation of both molecules, and symmetric under molecule exchange. By putting all these requirements together, $\mathcal{K}$ turns into a function $K(\Omega_{12})$ of the relative orientation Ω_{12} between the molecules. Moreover, $\mathcal{K}$ is to be invariant under the action of the symmetry group of either molecule. For biaxial molecules endowed with the D_{2h} symmetry, this requirement leads one to assume that $K(\Omega_{12})$ can be expanded on the following set of symmetry-adapted functions [21]:

$$\Delta^{(l)}_{m,n}(\Omega_{12}) := \left(\frac{\sqrt{2}}{2}\right)^{2+\delta_{m,0}+\delta_{n,0}} \sum_{\sigma,\sigma'=\{-1,1\}} \mathcal{D}^{(l)}_{\sigma m,\sigma' n}(\Omega_{12}),$$

$$l \text{ even}, 0 \leqslant m,\ n \leqslant l, \text{ even},$$

$$l \text{ odd}, 2 \leqslant m,\ n \leqslant l, \text{ even}, \tag{2.2}$$

where δ is Kronecker's delta, and $\mathcal{D}^{(l)}_{m,n}$ are Wigner's rotation matrices of order l, defined according to Sec. 13 of [22]. The functions Δ occurring in Eq. (2.2) form an orthogonal system since they obey the equations

$$\int \Delta^{(l)}_{m,n}(\Omega)\Delta^{(l')}_{m',n'}(\Omega)d\Omega = \frac{8\pi^2}{2l+1}\delta_{l,l'}\delta_{m,m'}\delta_{n,n'}.$$

Thus we can write the formal expansion of $K(\Omega_{12})$ as

$$K(\Omega_{12}) = \sum_{l,m,n} \frac{2l+1}{8\pi^2} K_{l,mn}\Delta^{(l)}_{m,n}(\Omega_{12}), \tag{2.3}$$

where the indices l, m, and n have the same range as in Eq. (2.2). By definition,

$$K_{l,mn}[K] := \int K(\Omega_{12})\Delta^{(l)}_{m,n}(\Omega_{12})d\Omega_{12}. \tag{2.4}$$

In the sequel, we will refer to the coefficients $K_{2,mn}$ as the quadrupolar projection of $K(\Omega_{12})$.

The orientational distribution function Ψ can be obtained by minimizing the functional $f[\Psi]$ in Eq. (2.1), under the constraint that

$$\int \Psi(\Omega)d\Omega = 1.$$

As a result, Ψ obeys the nonlinear integral equation

$$\Psi = \frac{\exp(-\eta K[\Psi])}{\int \exp(-\eta K[\Psi](\Omega))d\Omega}. \tag{2.5}$$

Solving Eq. (2.5) is a challenging and still open problem. However, since the isotropic distribution function $\Psi_0(\Omega) = \frac{1}{8\pi^2}$ solves Eq. (2.5), following Kayser and Raveché [23], Mulder [10] performed a bifurcation analysis of this equation around Ψ_0 assuming that the bifurcating solutions had the same symmetry as the interaction kernel K, and so could be written as

$$\Psi(\Omega) = \sum_{l,m,n} \frac{2l+1}{8\pi^2} \psi_{l,mn} \Delta^{(l)}_{m,n}(\Omega).$$

Mulder's analysis builds on the following hypothesis:

Solutions of Eq. (2.5) bifurcating from

$$\Psi_0 \text{ belong to the subspace } l = 2. \tag{2.6}$$

In fact, the subspace with $l=2$ is the smallest subspace that accommodates isotropic, uniaxial, and biaxial phases. As soon the hypothesis (2.6) is accepted, only the symmetry-adapted functions with $l=2$ are relevant: they are

$$\Delta^{(2)}_{0,0}(\Omega) := \frac{1}{2}(3\cos^2\vartheta - 1) = P_2(\cos\vartheta),$$

$$\Delta^{(2)}_{0,2}(\Omega) := \frac{\sqrt{3}}{2}\sin^2\vartheta\cos 2\psi,$$

$$\Delta^{(2)}_{2,0}(\Omega) := \frac{\sqrt{3}}{2}\sin^2\vartheta\cos 2\varphi,$$

$$\Delta^{(2)}_{2,2}(\Omega) := \frac{1}{2}(1+\cos^2\vartheta)\cos 2\varphi\cos 2\psi - \cos\vartheta\sin 2\varphi\sin 2\psi, \tag{2.7}$$

where $(\varphi, \vartheta, \psi)$ are the Euler angles associated with the relative orientation Ω_{12} of the interacting molecules, defined according to the y-notation (see pp. 606–608 of [24]), and P_2 is the second Legendre polynomial.

In the spirit of Onsager's theory [1], we identify $\mathcal{K}$ with the effective interaction Hamiltonian [8]. For hard-core interactions, $\mathcal{K}$ is the excluded volume between two interacting molecules. In Sec. III, we will determine the coefficients $K_{2,mn}$ of the excluded-volume interaction between spherocuboids, a rather general class of biaxial molecules.

III. EXCLUDED VOLUME

Building upon the monograph [16] and on Mulder's paper [19], we first recall the definition of a spherocuboid and we record the formula for the excluded volume between two equal spherocuboids; then we compute its quadrupolar projection. Let $\mathcal{P}$ be a parallelepiped with sides of length a, b, and c placed along a given set of orthogonal unit vectors $\{\boldsymbol{m}_1, \boldsymbol{m}_2, \boldsymbol{m}_3\}$ and let $\mathcal{B}$ be a ball of radius R. If the center of $\mathcal{B}$ is moved on the boundary $\partial\mathcal{P}$ of $\mathcal{P}$, the boundary of $\mathcal{B}$ will span the surface of a new body $\mathcal{SC}$ which inherits the central symmetry of $\mathcal{P}$: $\mathcal{SC}$ is called the spherocuboid generated by $\mathcal{P}$ (see Fig. 1). A formal definition of spherocuboids as a special case of spherozonotopes can be found in [19]. Here, we heed the reader that the construction of $\mathcal{SC}$ just sketched is a special case of *Minkowski addition* between convex bodies (see Chap. 2 of [16]). In [19], Mulder arrived at the exact expression for the excluded volume between spherozonotopes. To our purpose it is enough to adapt his general result to the case of two equal, arbitrarily oriented spherocuboids $\mathcal{SC}$ and $\mathcal{SC}'$, where $\mathcal{SC}'$ has the sides of length a, b, and c placed along a set $\{\boldsymbol{m}'_1, \boldsymbol{m}'_2, \boldsymbol{m}'_3\}$ of orthogonal unit vectors. The molecular axes $\{\boldsymbol{m}_1, \boldsymbol{m}_2, \boldsymbol{m}_3\}$ and $\{\boldsymbol{m}'_1, \boldsymbol{m}'_2, \boldsymbol{m}'_3\}$ will be oriented so that

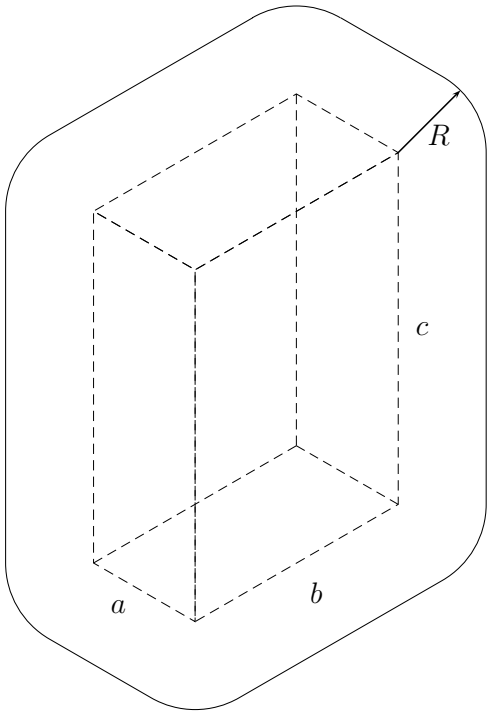

FIG. 1. Sketch of a spherocuboid obtained by Minkowski addition of a parallelepiped with sides of length a, b, and c, and a sphere of radius R.

$$\boldsymbol{m}_1 \times \boldsymbol{m}_2 \cdot \boldsymbol{m}_3 = \boldsymbol{m}'_1 \times \boldsymbol{m}'_2 \cdot \boldsymbol{m}'_3 = +1,$$

with the stipulation that $\boldsymbol{m}_3$ and $\boldsymbol{m}'_3$ represent the long molecular axes of the interacting molecules. Hereafter we shall assume, with no prejudice to generality, that $a \leqslant b \leqslant c$.

The excluded volume $\mathcal{E}[\mathcal{SC}, \mathcal{SC}']$ between $\mathcal{SC}$ and $\mathcal{SC}'$ can be expressed with the aid of Steiner's formula [19] as

$$\mathcal{E}[\mathcal{SC}, \mathcal{SC}'] = \mathcal{V} + 2\mathcal{A}R + 16\pi\mathcal{M}R^2 + \frac{32\pi}{3}R^3, \tag{3.1}$$

where

$$\mathcal{V} := b(a^2+c^2)[|\boldsymbol{m}_1\cdot\boldsymbol{m}_3'+\boldsymbol{m}_1'\cdot\boldsymbol{m}_3|]+c(a^2+b^2)$$
$$\times[|\boldsymbol{m}_1\cdot\boldsymbol{m}_2'+\boldsymbol{m}_1'\cdot\boldsymbol{m}_2|]+a(b^2+c^2)[|\boldsymbol{m}_2\cdot\boldsymbol{m}_3'+\boldsymbol{m}_3'\cdot\boldsymbol{m}_2|]$$
$$+2abc(1+|\boldsymbol{m}_1\cdot\boldsymbol{m}_1'|+|\boldsymbol{m}_2\cdot\boldsymbol{m}_2'|+|\boldsymbol{m}_3\cdot\boldsymbol{m}_3'|), \tag{3.2}$$

$$\mathcal{A} := 4(ab+bc+ac)+2[a^2|\boldsymbol{m}_1\cdot\boldsymbol{m}_1'|+b^2|\boldsymbol{m}_2\cdot\boldsymbol{m}_2'|$$
$$+c^2|\boldsymbol{m}_3\cdot\boldsymbol{m}_3'|]+2ab[|\boldsymbol{m}_1\times\boldsymbol{m}_2'|+|\boldsymbol{m}_2\times\boldsymbol{m}_1'|]$$
$$+2ac[|\boldsymbol{m}_1\times\boldsymbol{m}_3'|+|\boldsymbol{m}_3\times\boldsymbol{m}_1'|]$$
$$+2bc[|\boldsymbol{m}_2\times\boldsymbol{m}_3'|+|\boldsymbol{m}_3\times\boldsymbol{m}_2'|], \tag{3.3}$$

and

$$\mathcal{M} := \frac{1}{2}(a+b+c). \tag{3.4}$$

Two particular cases are worth noting. If $R=0$, spherocuboids coincide with Straley's platelets [8]. If $\mathcal{P}$ degenerates into a rectangular plate, spherocuboids coincide with spheroplatelets [17].

With the aid of the results recorded in Eqs. (A7)–(A15) of Appendix A, Eqs. (3.1)–(3.4) allow us to compute the quadrupolar projection of the excluded-volume interaction between two identical spherocuboids:

$$K_{2,00}^*[\mathcal{E}(\mathcal{SC},\mathcal{SC}')]$$
$$=\frac{1}{8}\left\{\left[-b(a^2+c^2)-a(b^2+c^2)+\frac{c}{2}(a^2+b^2)+3abc\right]\right.$$
$$\left.+\pi R\left[-\frac{1}{4}(a^2+b^2)-c^2+c(a+b)-\frac{1}{2}ab\right]\right\}, \tag{3.5}$$

$$K_{2,02}^*[\mathcal{E}(\mathcal{SC},\mathcal{SC}')]=K_{2,20}^*[\mathcal{E}(\mathcal{SC},\mathcal{SC}')]$$
$$=\frac{\sqrt{3}}{16}\left\{[b(a^2+c^2)-a(b^2+c^2)]\right.$$
$$\left.+\pi R\left[\frac{1}{2}(a^2-b^2)+c(b-a)\right]\right\}, \tag{3.6}$$

and

$$K_{2,22}^*[\mathcal{E}(\mathcal{SC},\mathcal{SC}')]=\frac{3}{16}\left\{[2abc-c(a^2+b^2)]\right.$$
$$\left.+\pi R\left[ab-\frac{1}{2}(a^2+b^2)\right]\right\}, \tag{3.7}$$

where

$$K_{2,mn}^* := \frac{1}{8\pi^2}K_{2,mn}.$$

Equations (3.5)–(3.7) contain as special limiting cases the results obtained by Mulder [10] for spheroplatelets. To recover Mulder's notation we set here $a=0$ and rename R as a in Eqs. (3.5)–(3.7), which then reduce to Eqs. (4.6) of [10]. Straley's platelets can also be obtained as special spheroplatelets by simply setting $R=0$ in Eqs. (3.5)–(3.7) and then renaming a, b, and c as B, W, and L, respectively, which stand for breadth, width, and length of the platelets. These transformations produce the following formulas:

$$K_{2,00}^{*S}=\frac{1}{16}[L(B^2+W^2)-2W(B^2+L^2)$$
$$-2B(W^2+L^2)+6BLW], \tag{3.8}$$

$$K_{2,02}^{*S}=K_{2,20}^{*S}=-\frac{\sqrt{3}}{16}[(L^2-BW)(B-W)], \tag{3.9}$$

and

$$K_{2,22}^{*S}=-\frac{3}{16}L[(W-B)^2], \tag{3.10}$$

which, apart from the multiplicative factor 15/16, agree with Eqs. (4.9) of [10], which amended Eqs. (9) of [8]. It is worth noting that Straley [8] obtained these equations by *interpolation* of the then unknown excluded volume of a pair of platelets with the most general quadrupolar function of the relative orientation compatible with the platelet symmetry. Precisely, Straley computed the excluded volume of a pair of platelets in some special relative orientations and then determined the coefficients $K_{2,mn}$ by requiring the general quadrupolar formula, that is, Eq. (2.3) with $l=2$, to take these very values of the excluded volume in the corresponding specific orientations. It is remarkable, but presumably accidental, that the coefficients $K_{2,mn}$ obtained here by projection are simply proportional to those obtained by interpolation.

IV. PARTLY REPULSIVE PROJECTION

Straley [8] wrote the general interaction Hamiltonian between two plateletlike molecules as a function of the Euler angles representing their relative orientation:

$$H=\alpha_S+\beta_S F_1(\vartheta)+\gamma_S[F_2(\vartheta,\varphi)+F_3(\vartheta,\psi)]+\delta_S F_4(\vartheta,\varphi,\psi), \tag{4.1}$$

where α_S, β_S, γ_S, and δ_S are scalar parameter, and the functions F_i are related to the symmetrized functions $\Delta_{m,n}^{(2)}$ by

$$F_1(\vartheta)=\Delta_{0,0}^{(2)},\quad F_2(\vartheta,\varphi)=-\frac{2}{\sqrt{3}}\Delta_{2,0}^{(2)},$$

$$F_3(\vartheta,\psi)=-\frac{2}{\sqrt{3}}\Delta_{0,2}^{(2)},\quad F_4(\vartheta,\varphi,\psi)=\Delta_{2,2}^{(2)},$$

where the negative signs mirror the different notations followed by Straley and Mulder in defining the Euler angles: the x-notation instead of the y-notation. Straley's model has been reformulated by the use of two tensors, $\mathbf{q}$ and $\mathbf{b}$, that decompose the molecular polarization [11]:

$$\mathbf{q} := \boldsymbol{m}_3\otimes\boldsymbol{m}_3-\frac{1}{3}\mathbf{I},$$

and

$$\mathbf{b} := \boldsymbol{m}_1\otimes\boldsymbol{m}_1-\boldsymbol{m}_2\otimes\boldsymbol{m}_2,$$

where $\mathbf{I}$ is the identity. In terms of these tensors, Straley's Hamiltonian can be written as [25]

$$H = -U_0\{\xi(\mathbf{q}\cdot\mathbf{q}') + \gamma(\mathbf{q}\cdot\mathbf{b}' + \mathbf{q}'\cdot\mathbf{b}) + \lambda(\mathbf{b}\cdot\mathbf{b}')\}, \tag{4.2}$$

where the pairs $(\mathbf{q},\mathbf{b})$ and $(\mathbf{q}',\mathbf{b}')$ represent two interacting molecules. $U_0>0$ sets the *strength* of the interaction, and the parameters ξ, γ, and λ do not exceed 1 in magnitude. With no loss of generality, we can assume $\xi=1$ [12]. As shown in [11], requiring H to attain its minimum for $(\mathbf{q},\mathbf{b})=(\mathbf{q}',\mathbf{b}')$, where the interacting molecules are parallel to one another, amounts to restricting the (γ,λ)-plane to the admissible fan-shaped region defined by

$$\lambda > 0 \quad \text{and} \quad \lambda - |2\gamma| + 1 > 0. \tag{4.3}$$

It is shown in [12] that H in Eq. (4.2) can be recast in the form

$$H = -U\{a^+\mathbf{q}^+\cdot\mathbf{q}^{+\prime} + a^-\mathbf{q}^-\cdot\mathbf{q}^{-\prime}\}, \tag{4.4}$$

where $\mathbf{q}^+$ and $\mathbf{q}^-$ are orthogonal tensors depending on γ and λ that realize a different decomposition of the molecular polarizability. When both $a^\pm$ are positive, H results in the superposition of two attractive London interactions, and it is said *fully attractive*. When either a^+ or a^- is negative, H possesses both attractive and repulsive components and it is said *partly repulsive*. All partly repulsive interactions fall below the dispersion parabola

$$\lambda < \gamma^2, \tag{4.5}$$

whereas all fully attractive interactions fall above it: $\lambda>\gamma^2$ [12]. All partly repulsive interactions have a common feature: they give rise to qualitatively the same phase diagram, which predicts the direct isotropic-to-biaxial transition to happen at a single Landau point. This phase diagram, which has long been known [9], is precisely the same predicted for purely dispersive London interactions described by the parabola $\lambda=\gamma^2$ [26,27]. For a general partly repulsive interaction the Landau point in the phase diagram occurs only along the lines [12]

$$3\lambda + 2|\gamma| - 1 = 0, \tag{4.6}$$

in accordance with the results of Mulder [10].

Here we show that the quadrupolar projection of the excluded-volume interaction for spherocuboids arrived at in the preceding section is partly repulsive for all choices of the geometric parameters $a\leqslant b\leqslant c$. Studying all pairs (γ,λ) in the admissible set (4.3) is indeed redundant. As discussed in [25,28], since the molecular interaction is not affected by relabeling the molecular axes, the parameters in the interaction potential can be restricted to the *essential triangle* bounded by the lines

$$\gamma = 0, \quad \lambda = 0, \quad 2\gamma + 3\lambda - 1 = 0, \tag{4.7}$$

or to any of its images under the set of symmetry transformations that relabel the molecular axes [see also [29] for a systematic account on the symmetries enjoyed by H in Eq. (4.2)]. One of these images, depicted in Fig. 2, is obtained by reflecting the essential triangle about the λ axis. We write the quadrupolar projection K_2 of the excluded-volume interaction between spherocuboids as

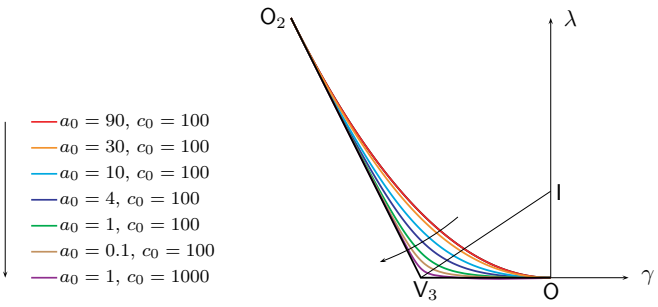

FIG. 2. (Color online) A set of curves $(\Gamma(a_0,b,c_0),\Lambda(a_0,b,c_0))$ are plotted here, for several values of a_0 and c_0. The arrows indicate the correspondence between curves and pairs (a_0,c_0). All these curves pass through the point $\mathsf{O}=(0,0)$ for $b=a$, and through the point $\mathsf{O}_2=(-1,1)$ for $b=c$. As proved in Appendix C, the curves $(\Gamma(a_0,b,c_0),\Lambda(a_0,b,c_0))$ cover the region $\mathsf{OO}_2\mathsf{V}_3$ below the dispersion parabola $\lambda=\gamma^2$. OIV_3 is the image of the essential triangle bounded by the lines (4.7). $\mathsf{I}=\left(0,\frac{1}{3}\right)$ and $\mathsf{V}_3=\left(-\frac{1}{2},0\right)$.

$$K_2 := 5[K^*_{2,00}\Delta^{(2)}_{0,0}(\Omega_{12}) + K^*_{2,02}\Delta^{(2)}_{0,2}(\Omega_{12}) + K^*_{2,20}\Delta^{(2)}_{2,0}(\Omega_{12}) + K^*_{2,22}\Delta^{(2)}_{2,2}(\Omega_{12})].$$

Comparing this formula and Eq. (4.1), we make the following identifications:

$$\beta_S = -\frac{2}{3}U_0\xi = 5K^*_{2,00}, \quad \gamma_S = -U_0\gamma = \frac{5\sqrt{3}}{2}K^*_{2,02} = \frac{5\sqrt{3}}{2}K^*_{2,20}, \quad \delta_S = -2U_0\lambda = 5K^*_{2,22}, \tag{4.8}$$

whence it follows that

$$\lambda = \frac{1}{3}\frac{K^*_{2,22}}{K^*_{2,00}}, \quad \gamma = \frac{1}{\sqrt{3}}\frac{K^*_{2,02}}{K^*_{2,00}}. \tag{4.9}$$

The admissible region (4.3) in the (γ,λ)-plane is thus mapped into the region in the $K^*_{2,mn}$-space defined by the inequalities

$$\frac{K^*_{2,22}}{K^*_{2,00}} > 0, \quad \frac{K^*_{2,22} - 2\sqrt{3}K^*_{2,02} + 3K^*_{2,00}}{3K^*_{2,00}} > 0, \quad \text{and} \quad \frac{K^*_{2,22} + 2\sqrt{3}K^*_{2,02} + 3K^*_{2,00}}{3K^*_{2,00}} > 0, \tag{4.10}$$

and the region (4.5) is mapped into

$$K^*_{2,00}K^*_{2,22} < (K^*_{2,02})^2. \tag{4.11}$$

Moreover, by setting $\xi=1$ in Eq. (4.2), we see from the first of Eqs. (4.8) that U_0 is positive if and only if $K^*_{2,00}$ is negative.

It is convenient to scale all dimensions of a spherocuboid to πR, thus introducing the formal transformations

$$a \mapsto \frac{a}{\pi R}, \quad b \mapsto \frac{b}{\pi R}, \quad c \mapsto \frac{c}{\pi R}. \tag{4.12}$$

Using these in Eqs. (3.5)–(3.7) multiplied by $16/(\pi R)^3$ we transform $K^*_{2,mn}$ into functions of (a,b,c), which we denote by $k_{2,mn}$:

$$k_{2,00}(a,b,c) = \left\{ [-2b(a^2+c^2) - 2a(b^2+c^2) + c(a^2+b^2) + 6abc] + \left[2c(a+b) - \frac{1}{2}(a+b)^2 - 2c^2 \right] \right\}, \tag{4.13}$$

$$k_{2,02}(a,b,c) = k_{2,20}(a,b,c) = \sqrt{3}\left\{ [b(a^2+c^2) - a(b^2+c^2)] + \left[\frac{1}{2}(a^2-b^2) + c(b-a) \right] \right\}, \tag{4.14}$$

and

$$k_{2,22}(a,b,c) = -3\frac{2c+1}{2}(a-b)^2. \tag{4.15}$$

The quadrupolar projection of the excluded volume is meaningful whenever the coefficients $K_{2,00}$, $K_{2,02}$, and $K_{2,22}$ are not all zero. It can be checked that the functions (4.13)–(4.15) all vanish only for $a=b=c$, in which case the molecules possess a cubatic D_{4h} symmetry. This case cannot be fully treated within the quadrupolar approximation to the excluded-volume interaction, as also confirmed by another fairly recent analysis with different molecules enjoying this symmetry [30]. Inserting functions (4.13)–(4.15) into Eqs. (4.9) instead of $K^*_{2,mn}$, we express γ and λ as functions of (a,b,c), which we denote by $\Lambda(a,b,c)$ and $\Gamma(a,b,c)$, respectively.

Use of Eqs. (4.13)–(4.15) into Eq. (4.11) gives this the following form:

$$(k_{2,02})^2 - k_{2,00}k_{2,22} = 3(a-b)^2(a-c)^2(b-c)^2 > 0. \tag{4.16}$$

Thus the quadrupolar projection of the excluded-volume interaction between spherocuboids never lies above the dispersion parabola $\lambda=\gamma^2$; it lies on this parabola only when two sides of the parallelepiped $\mathcal{P}$ have equal length and the corresponding spherocuboid enjoys a higher symmetry. Only specific points on the dispersion parabola can be attained: precisely,

$$\Gamma(a,a,c) = \Lambda(a,a,c) = 0, \tag{4.17}$$

$$\Gamma(a,c,c) = -1, \Lambda(a,c,c) = 1, \tag{4.18}$$

$$\Gamma(a,b,a) = \Lambda(a,b,a) = 1, \tag{4.19}$$

where the dispersion parabola $\lambda=\gamma^2$ is tangent to the boundary (4.3) of the admissible region (see Fig. 2). A glance at Eq. (4.15) suffices to conclude that $\lambda \geqslant 0$ whenever $U_0>0$, the equality being attained if and only if $a=b$, that is, at the origin of the (γ,λ)-plane. Even at the special points (4.17)–(4.19), where the quadrupolar interaction is uniaxial [12], the sphero-cuboids fail to be rotationally symmetric: the classical choice of Onsager's cylinders can only be recovered in an asymptotic limit (see Appendix B).

Since

$$k_{2,22} - 2\sqrt{3}k_{2,02} + 3k_{2,00} = -6(2b+1)(a-c)^2 \leqslant 0$$

and

$$k_{2,22} + 2\sqrt{3}k_{2,02} + 3k_{2,00} = -6(2b+1)(b-c)^2 \leqslant 0,$$

we conclude that, when $U_0>0$, the quadrupolar projection of the excluded-volume interaction between spherocuboids always lies within the admissible region (4.3). Actually, the admissible region below the dispersion parabola is fully covered by the mappings $\Gamma(a,b,c)$ and $\Lambda(a,b,c)$, as is shown pictorially in Fig. 2 and proved analytically in Appendix C.

Two further limiting cases deserve notice. One such case is the line $3\lambda-2\gamma-1=0$ inhabited by Landau points on the phase diagram [12]. By Eq. (4.9), it corresponds to the following "geometric mean" relation among the scaled sizes of the spherocuboid:

$$2b+1 = \sqrt{2a+1}\sqrt{2c+1}. \tag{4.20}$$

This equation extends to spherocuboids Eq. (4.8) found in [10] for spheroplatelets. The other case is the limit as R decreases to 0: it represents Straley's platelets, but cannot be formally retraced here because of the normalization chosen in Eq. (4.12). This case is examined separately in Appendix D.

V. CONCLUSIONS

The effective quadrupolar molecular interaction put forward by Straley [8] has recently shown the ability to describe some subtle features in the phase diagram of new thermotropic biaxial phases [31], such as the presence of a tricritical point along the uniaxial-to-biaxial transition line and the occurrence of a nonsingular, direct isotropic-to-biaxial transition [11,25,32]. The general mean-field quadrupolar model for biaxial nematics has been solved in [12], where all admissible effective Hamiltonians have been classified as either fully attractive or partly repulsive, as to whether they can be resolved in two London attractors or in a London attractor and a London "repulsor." Intuition suggests that the excluded-volume interactions between biaxial hard particles are the natural candidates to provide examples of partly repulsive interactions, much in the spirit of Straley's platelets [8]. Here we explored this possibility within the class of spherocuboids, for which Mulder [19] has recently made the excluded volume accessible.

We proved that the quadrupolar projection of the excluded volume for all spherocuboids falls within the partly repulsive region, which in the parametrization (4.2) of the approximating Hamiltonian is the region $\lambda<\gamma^2$ below the purely London dispersion parabola [12]. More precisely, we showed that the whole partly repulsive region within the stability range (4.3) of the approximating quadrupolar Hamiltonian is completely covered upon varying the geometric parameters of spherocuboids. We are led by this result to conjecture that this is indeed a characteristic property of the quadrupolar projection of the excluded-volume interaction between all hard particles with the D_{2h} symmetry.

In the light of the mean-field analysis of the general dispersion quadrupolar model for biaxial nematics [12], the conclusion we arrived at is more than a mere computation. Dispersion and excluded-volume interactions live, as it were, in different worlds, as do the statistical theories based upon them: thermal the former, athermal the latter. However, a bridge can be established between these theories, which is somewhat formal in nature, through the quadrupolar approximation to the effective Hamiltonians. This has been our major concern here. The mean-field analysis of the general dispersion quadrupolar model [12] exhibits a rich variety of phase transitions, including both first- and second-order isotropic-to-biaxial transitions. These latter are displayed only for values of the parameters that make the Hamiltonian fully attractive. By contrast, we showed that the parameters that pertain to the effective quadrupolar Hamiltonian generated by the excluded-volume interaction of equal spherocuboids make it partly repulsive.

Since all partly repulsive quadrupolar Hamiltonians feature one and the same phase diagram, where the isotropic-to-biaxial transition takes place at a single Landau point, we expect that this property also applies to the general excluded-volume interaction for equal spherocuboids, if the knowledge of the quadrupolar coefficients of a biaxial interaction is to determine qualitatively the equilibrium bifurcation scenarios [10]. A computer simulation of the complete excluded-volume interaction between spherocuboids could help establish this result. In particular, the occurrence of a direct isotropic-to-biaxial transition that we predict whenever Eq. (4.20) is obeyed should be subjected to further scrutiny. Cubatic phases will presumably escape our prediction, as spherocuboids possess the D_{4h} symmetry only when the quadrupolar approximation to the excluded-volume interaction vanishes identically.

In general, it would be naïve to expect that all qualitative features of the phase diagram established in [12] for the quadrupolar Hamiltonian H apply to a full excluded-volume computation. In particular, the isotropic-to-uniaxial transition could also become second-order. Eq. (4.20), on the contrary, seems to reveal a symmetry of the excluded-volume interaction, brought into the open by the structure of the effective quadrupolar Hamiltonian. If truly based on symmetry, our prediction should not depend on the approximation employed to formulate it.

APPENDIX A: QUADRUPOLAR COEFFICIENTS

Here we compute the coefficients of the quadrupolar projection for the excluded volume of two identical spherocuboids defined in Eq. (2.4). We display the strategy outlined in the Appendix of [10].

The main technical difficulty in computing these coefficients arises from the presence of absolute values in Eqs. (3.2)–(3.4). Mulder [10] noted that for any two arbitrary rotations $\mathbf{R}_1$ and $\mathbf{R}_2$, given a function $f(\Omega_{12})$ of the relative orientation between two particles, the following identity follows:

$$\int f(\Omega_{12})\Delta^{(2)}_{m,n}(\Omega_{12})d\Omega_{12} = \int g(\tilde{\Omega}_{12})\Delta^{(2)}_{m,n}(\tilde{\Omega}_{12})d\tilde{\Omega}_{12}. \tag{A1}$$

Here $\tilde{\Omega}_{12}$ is the set of Euler angles representing the rotation $\mathbf{R}_1\mathbf{R}_{12}\mathbf{R}_2^{-1}$, where $\mathbf{R}_{12}$ is the relative rotation represented by Ω_{12}, and g is related to f through

$$f(\Omega_{12}) = g(\tilde{\Omega}_{12}). \tag{A2}$$

By the closure properties of Wigner's matrices (see p. 122 of [33]), we also have that

$$\Delta^{(2)}_{m,n}(\tilde{\Omega}_{12}) := \Delta^{(2)}_{m,p}(\Omega_1)\Delta^{(2)}_{n,q}(\Omega_2)\Delta^{(2)}_{p,q}(\Omega_{12}), \tag{A3}$$

where Ω_1 and Ω_2 denote the sets of Euler angles representing $\mathbf{R}_1$ and $\mathbf{R}_2$, respectively, and summations over the appropriate ranges of p and q are implied. The advantage of this approach is that, by a judicious choice of the rotations $\mathbf{R}_1$ and $\mathbf{R}_2$, we can eventually reduce the computation of the general coefficients $K_{2,mn}[\mathcal{E}[\mathcal{SC},\mathcal{SC}']]$ to the much easier computation of the coefficients $K_{2,mn}[|\boldsymbol{m}_3\cdot\boldsymbol{m}_3'|]$ and $K_{2,mn}[|\boldsymbol{m}_3\times\boldsymbol{m}_3'|]$.

In particular,

$$\begin{aligned} K_{2,00}[|\boldsymbol{m}_3\cdot\boldsymbol{m}_3'|] &= \int |\boldsymbol{m}_3\cdot\boldsymbol{m}_3'|\Delta^{(2)}_{0,0}(\Omega_{12})d\Omega_{12} \\ &= \int_0^{2\pi} d\psi \int_0^{2\pi} d\varphi \int_0^{\pi} \sin\vartheta|\cos\vartheta|P_2 \\ &\quad \times(\cos\vartheta)d\vartheta \\ &= 4\pi^2\int_{-1}^{1}\frac{|x|}{2}(3x^2-1)dx = \pi^2, \end{aligned}$$

where the change of variable $x=\cos\vartheta$ has also been made. It is readily seen from Eq. (2.7) that $K_{2,mn}[|\boldsymbol{m}_3\cdot\boldsymbol{m}_3'|]$ vanishes identically if either m or n are different from zero. Similarly,

$$K_{2,00}[|\boldsymbol{m}_3\times\boldsymbol{m}_3'|] = 4\pi^2\int_{-1}^{1}P_2(x)\sqrt{1-x^2}dx = -\frac{\pi^3}{4}$$

is the only $K_{2,mn}[|\boldsymbol{m}_3\cdot\boldsymbol{m}_3'|]$ that does not vanish.

We now reduce all remaining coefficients to those already computed. In the y-notation for Euler angles the rotation $\mathbf{R}_1$ by $\pi/2$ around $\boldsymbol{m}_1$, which maps $\boldsymbol{m}_2$ into $\boldsymbol{m}_3$ and $\boldsymbol{m}_3$ into $-\boldsymbol{m}_2$, is represented by $\vartheta_1=-\pi/2$, $\varphi_1=\pi/2$, and $\psi_1=\pi/2$, while the rotation $\mathbf{R}_2$ by $\pi/2$ around $\boldsymbol{m}_2$, which maps $\boldsymbol{m}_1$ into $-\boldsymbol{m}_3$ and $\boldsymbol{m}_3$ into $\boldsymbol{m}_1$, is represented by $\vartheta_2=\pi/2$, $\varphi_2=\psi_2=0$. By use of Eq. (2.7) we obtain

$$\Delta^{(2)}_{0,0}(\Omega_1) = -\frac{1}{2},\quad \Delta^{(2)}_{0,2}(\Omega_1) = \Delta^{(2)}_{2,0}(\Omega_1) = -\frac{\sqrt{3}}{2},\quad \Delta^{(2)}_{2,2}(\Omega_1) = \frac{1}{2}, \tag{A4}$$

$$\Delta^{(2)}_{0,0}(\Omega_2) = -\frac{1}{2}, \quad \Delta^{(2)}_{0,2}(\Omega_2) = \Delta^{(2)}_{2,0}(\Omega_2) = \frac{\sqrt{3}}{2}, \quad \Delta^{(2)}_{2,2}(\Omega_2) = \frac{1}{2}. \tag{A5}$$

Finally, when either $\mathbf{R}_1$ or $\mathbf{R}_2$ is the identity $\mathbf{I}$, $\Omega_i \equiv 0$ and

$$\Delta^{(2)}_{0,0}(0) = 1, \quad \Delta^{(2)}_{0,2}(0) = \Delta^{(2)}_{2,0}(0) = 0, \quad \Delta^{(2)}_{2,2}(0) = 1. \tag{A6}$$

To illustrate better this computational strategy, we consider, for instance, the term $|\boldsymbol{m}_2 \cdot \boldsymbol{m}_1'| = |\mathbf{R}_1 \boldsymbol{m}_3 \cdot \mathbf{R}_2 \boldsymbol{m}_3'|$. By Eqs. (A1)–(A3) with $m=n=0$, we can write

$$\int |\boldsymbol{m}_2 \cdot \boldsymbol{m}_1'| \Delta^{(2)}_{0,0}(\tilde{\Omega}_{12}) d\tilde{\Omega}_{12} = \int |\boldsymbol{m}_3 \cdot \boldsymbol{m}_3'| \Delta^{(2)}_{0,p}(\Omega_1) \Delta^{(2)}_{0,q}(\Omega_2) \Delta^{(2)}_{p,q}(\Omega_{12}) d\Omega_{12}.$$

Since $|\boldsymbol{m}_3 \cdot \boldsymbol{m}_3'| = |\cos\vartheta|$, it follows from Eqs. (2.7) that only the term with $p=q=0$ contributes to the last integral, and so, by Eqs. (A4) and (A5),

$$K_{2,00}[|\boldsymbol{m}_2 \cdot \boldsymbol{m}_1'|] = \int |\boldsymbol{m}_2 \cdot \boldsymbol{m}_1'| \Delta^{(2)}_{0,0}(\tilde{\Omega}_{12}) d\tilde{\Omega}_{12} = 4\pi^2 \int_{-1}^{1} \frac{1}{4} |\cos\vartheta| \Delta^{(2)}_{0,0}(\Omega_{12}) d\Omega_{12} = \frac{\pi^2}{4}.$$

Similarly,

$$\Delta^{(2)}_{0,2}(\tilde{\Omega}_{12}) = \Delta^{(2)}_{2,0}(\tilde{\Omega}_{12}) = \Delta^{(2)}_{0,p}(\Omega_1) \Delta^{(2)}_{2,q}(\Omega_2) \Delta^{(2)}_{p,q}(\Omega_{12}) = \Delta^{(2)}_{0,0}(\Omega_1) \Delta^{(2)}_{2,0}(\Omega_2) \Delta^{(2)}_{0,0}(\Omega_{12}) + \text{z.m.t.},$$

where by z.m.t. we denote terms with zero mean, which do not contribute to $K_{2,mn}$. Hence

$$K_{2,02}[|\boldsymbol{m}_2 \cdot \boldsymbol{m}_1'|] = K_{2,20}[|\boldsymbol{m}_2 \cdot \boldsymbol{m}_1'|] = 4\pi^2 \int |\boldsymbol{m}_3 \cdot \boldsymbol{m}_3'| \Delta^{(2)}_{20}(\Omega_1) \Delta^{(2)}_{20}(\Omega_2) \times \Delta^{(2)}_{00}(\Omega_{12}) d\Omega_{12} = 4\pi^2 \int_{-1}^{1} \frac{1}{4} |\cos\vartheta| \Delta^{(2)}_{0,0}(\Omega_{12}) d\Omega_{12} = -\frac{\sqrt{3}}{4}.$$

Finally,

$$K_{2,22}[|\boldsymbol{m}_2 \cdot \boldsymbol{m}_1'|] = \int |\boldsymbol{m}_2 \cdot \boldsymbol{m}_1'| \Delta^{(2)}_{2,2}(\tilde{\Omega}_{12}) d\tilde{\Omega}_{12} = 4\pi^2 \int |\boldsymbol{m}_3 \cdot \boldsymbol{m}_3'| \Delta^{(2)}_{2,0}(\Omega_1) \Delta^{(2)}_{2,0}(\Omega_2) \times \Delta^{(2)}_{0,0}(\Omega_{12}) d\Omega_{12} = -\frac{3\pi^2}{4}.$$

For completeness, we also record the computations needed for $|\boldsymbol{m}_1 \times \boldsymbol{m}_3'| = |\mathbf{R}_2 \boldsymbol{m}_3 \times \mathbf{I} \boldsymbol{m}_3'|$. In this case $\mathbf{R}_1 = \mathbf{I}$ and

$$\Delta^{(2)}_{0,0}(\tilde{\Omega}_{12}) = \Delta^{(2)}_{0,0}(\Omega_2) \Delta^{(2)}_{0,0}(0) \Delta^{(2)}_{0,0}(\Omega_{12}) + \text{z.m.t.},$$

whence it follows that

$$K_{2,00}[|\boldsymbol{m}_1 \times \boldsymbol{m}_3'|] = -\frac{1}{2} \int |\boldsymbol{m}_3 \times \boldsymbol{m}_3'| \Delta^{(2)}_{0,0}(\Omega_{12}) d\Omega_{12} = -2\pi^2 \int_{-1}^{1} P_2(x) \sqrt{1-x^2} dx = \frac{\pi^3}{8}.$$

By Eq. (A6), it is now easy to check that

$$K_{2,02}[|\boldsymbol{m}_1 \times \boldsymbol{m}_3'|] = K_{2,20}[|\boldsymbol{m}_1 \times \boldsymbol{m}_3'|] = K_{2,22}[|\boldsymbol{m}_1 \times \boldsymbol{m}_3'|] = 0.$$

In Table I we collect the coefficients $K^*_{2,mn} := K_{2,mn}/8\pi^2$ for all the terms involved through Eqs. (3.1)–(3.4) in the excluded-volume interaction. This table is the extended version of Table 1 in [10] that was used to compute the quadrupolar projection of the excluded-volume interaction between spheroplatelets: compared to that table, ours involves only two basic families of integrals, instead of three.

Inspection of Table I yields the following three sets of formulas recorded here for use in Sec. III:

$$K^*_{2,00}[\mathcal{V}] = -\frac{b}{8}(a^2+c^2) - \frac{a}{8}(b^2+c^2) + \frac{c}{16}(a^2+b^2) + \frac{3}{8}abc, \tag{A7}$$

$$K^*_{2,00}[\mathcal{A}] = -\frac{\pi}{16}\left[\frac{1}{4}(a^2+b^2) + c^2 - c(a+b) + \frac{1}{2}bc\right], \tag{A8}$$

$$K^*_{2,00}[\mathcal{M}] = 0; \tag{A9}$$

$$K^*_{2,02}[\mathcal{V}] = K^*_{2,20}[\mathcal{V}] = \frac{\sqrt{3}}{16}[(b(a^2+c^2) - a(b^2+c^2)], \tag{A10}$$

$$K^*_{2,02}[\mathcal{A}] = K^*_{2,20}[\mathcal{A}] = \frac{\sqrt{3}\pi}{32}\left[\frac{1}{4}(a^2-b^2) + c(b-a)\right], \tag{A11}$$

$$K^*_{2,02}[\mathcal{M}] = K^*_{2,20}[\mathcal{M}(\mathcal{SC})] = 0, \tag{A12}$$

$$K^*_{2,22}[\mathcal{V}] = \frac{3}{16}[2abc - c(a^2+b^2)], \tag{A13}$$

$$K^*_{2,22}[\mathcal{A}] = \frac{3\pi}{32}\left[ab - \frac{1}{2}(a^2+b^2)\right], \tag{A14}$$

$$K^*_{2,22}[\mathcal{M}] = 0. \tag{A15}$$

APPENDIX B: ONSAGER'S CYLINDERS

The formalism developed by Mulder [19] makes it possible to obtain in a systematic way the classical result of

TABLE I. The coefficients $K^*_{2,mn} := K_{2,mn}/8\pi^2$ are tabulated for all the terms involved through Eqs. (3.1)–(3.4) in the excluded-volume interaction.

	$K^*_{2,00}$	$K^*_{2,02}$	$K^*_{2,20}$	$K^*_{2,22}$
$\lvert\boldsymbol{m}_3\cdot\boldsymbol{m}'_3\rvert$	$\frac{1}{8}$	0	0	0
$\lvert\boldsymbol{m}_3\cdot\boldsymbol{m}'_2\rvert$	$-\frac{1}{16}$	$-\frac{\sqrt{3}}{16}$	0	0
$\lvert\boldsymbol{m}_3\cdot\boldsymbol{m}'_1\rvert$	$-\frac{1}{16}$	$\frac{\sqrt{3}}{16}$	0	0
$\lvert\boldsymbol{m}_2\cdot\boldsymbol{m}'_3\rvert$	$-\frac{1}{16}$	0	$-\frac{\sqrt{3}}{16}$	0
$\lvert\boldsymbol{m}_2\cdot\boldsymbol{m}'_2\rvert$	$\frac{1}{32}$	$\frac{\sqrt{3}}{32}$	$\frac{\sqrt{3}}{32}$	$\frac{3}{32}$
$\lvert\boldsymbol{m}_2\cdot\boldsymbol{m}'_1\rvert$	$\frac{1}{32}$	$-\frac{\sqrt{3}}{32}$	$\frac{\sqrt{3}}{32}$	$-\frac{3}{32}$
$\lvert\boldsymbol{m}_1\cdot\boldsymbol{m}'_3\rvert$	$-\frac{1}{16}$	0	$\frac{\sqrt{3}}{16}$	0
$\lvert\boldsymbol{m}_1\cdot\boldsymbol{m}'_2\rvert$	$\frac{1}{32}$	$\frac{\sqrt{3}}{32}$	$-\frac{\sqrt{3}}{32}$	$-\frac{3}{32}$
$\lvert\boldsymbol{m}_1\cdot\boldsymbol{m}'_1\rvert$	$\frac{1}{32}$	$-\frac{\sqrt{3}}{32}$	$-\frac{\sqrt{3}}{32}$	$\frac{3}{32}$
$\lvert\boldsymbol{m}_3\times\boldsymbol{m}'_3\rvert$	$-\frac{\pi}{32}$	0	0	0
$\lvert\boldsymbol{m}_3\times\boldsymbol{m}'_2\rvert$	$\frac{\pi}{64}$	$\frac{\pi}{64}\sqrt{3}$	0	0
$\lvert\boldsymbol{m}_3\times\boldsymbol{m}'_1\rvert$	$\frac{\pi}{64}$	$-\frac{\pi}{64}\sqrt{3}$	0	0
$\lvert\boldsymbol{m}_2\times\boldsymbol{m}'_3\rvert$	$\frac{\pi}{64}$	0	$\frac{\pi}{64}\sqrt{3}$	0
$\lvert\boldsymbol{m}_2\times\boldsymbol{m}'_2\rvert$	$-\frac{\pi}{128}$	$-\frac{\pi}{128}\sqrt{3}$	$-\frac{\pi}{128}\sqrt{3}$	$-\frac{3\pi}{128}$
$\lvert\boldsymbol{m}_2\times\boldsymbol{m}'_1\rvert$	$-\frac{\pi}{128}$	$\frac{\pi}{128}\sqrt{3}$	$-\frac{\pi}{128}\sqrt{3}$	$\frac{3\pi}{128}$
$\lvert\boldsymbol{m}_1\times\boldsymbol{m}'_3\rvert$	$\frac{\pi}{64}$	0	$-\frac{\pi}{64}\sqrt{3}$	0
$\lvert\boldsymbol{m}_1\times\boldsymbol{m}'_2\rvert$	$-\frac{\pi}{128}$	$-\frac{\pi}{128}\sqrt{3}$	$\frac{\pi}{128}\sqrt{3}$	$\frac{3\pi}{128}$
$\lvert\boldsymbol{m}_1\times\boldsymbol{m}'_1\rvert$	$-\frac{\pi}{128}$	$\frac{\pi}{128}\sqrt{3}$	$\frac{\pi}{128}\sqrt{3}$	$-\frac{3\pi}{128}$

Onsager [1] for the excluded volume between two cylindric molecules of diameter d and height ℓ. In fact, a cylinder can be approximated in the Hausdorff metric (see Sec. 18 of [16]) by prisms of height ℓ with a regular polygon of $2N$ sides as a basis, inscribed into a circle of diameter d. If ϑ is the relative orientation between two congruent cylinders $\mathcal{C}$ and $\mathcal{C}'$, their excluded volume is [cf. Eq. (70) of [19]]

$$\frac{\pi}{2}\ell d^2 + \frac{\pi}{2}d(d^2+\ell^2)\sin\vartheta + \frac{\pi}{2}\ell d^2|\cos\vartheta| + 2\ell d^2 E(\sin\vartheta),$$

where

$$E(\sin\vartheta) := \int_0^{\pi/2} (1-\sin^2\vartheta\sin^2 t)^{1/2} dt$$

is the complete elliptic integral of the second kind. Clearly, in this case only the coefficient $K^*_{2,00}$ is not trivial and, by setting

$$\delta := \int_{-1}^{1} P_2(x)\left[\int_0^{\pi/2}[1-(1-x^2)\sin^2\varphi]^{1/2}d\varphi\right]dx \simeq 0.7011,$$

we arrive at

$$K^*_{2,00} = 4\pi^2 d^3\left[-\frac{\pi^2}{32}(1+\varrho^2)+\delta\varrho\right],$$

where $\varrho := \ell/d$. It can be checked by direct computation that $K^*_{2,00}<0$, and so $U_0>0$, if either

$$\varrho < 0.1159 \text{ or } \varrho > 2.1574.$$

In particular, the latter is obeyed in the limit of elongated cylinders, for which $\varrho \gg 1$.

APPENDIX C: COVERING CURVES

To see how the portion of the admissible region (4.3) that obeys (4.5) is covered by the mappings $\Gamma(a,b,c)$ and $\Lambda(a,b,c)$, we consider the curves in the (γ,λ)-plane parameterized as

$$[\Gamma(a_0,b,c_0),\Lambda(a_0,b,c_0)] \tag{C1}$$

for fixed values of a_0 and $c_0>a_0$. Precisely, we now prove that the region below the parabola $\lambda=\gamma^2$ that lies within the triangle bounded by the lines

$$\gamma=0, \quad \lambda=0, \quad -2\gamma+3\lambda-1=0$$

can be covered by curves in the family (C1). When $b\in[a_0,c_0]$, all curves in this family are constrained to pass through the points (0,0) and (−1,1) of the (γ,λ) plane. In particular, consider the case where $a_0=c_0-h$, with $h\ll 1$. Along these curves,

$$\Lambda(c_0-h,b,c_0)-\Gamma^2(c_0-h,b,c_0) = -\frac{4h^2}{(1+2c)^2}+O(h^3), \tag{C2}$$

and so they approach the limiting dispersion parabola $\lambda=\gamma^2$ to within any desired accuracy. To see why this parabola cannot be crossed by the quadrupolar projection of the excluded-volume interaction between spherocuboids, we

study the function $k_{2,00}(c_0-h,b,c_0)$, for $b=c_0-\varepsilon$, where $\varepsilon \ll 1$. By expanding (4.13) we obtain

$$k_{2,00}(c_0-h,c_0-\varepsilon,c_0) = -\frac{1}{2}(1+2c)\varepsilon^2 + (1+2b)h\varepsilon - \frac{h^2}{2}(2c+1) + O(3),$$

where $O(3)$ denotes terms that contain powers of h and ε of order 3, at least. Thus since $k_{2,00}$ is proportional to U_0, by Eq. (C1) the interaction strength tends to vanish when the point (Γ,Λ) approaches the dispersion parabola.

To see how the point (Γ,Λ) can reach the γ axis we first set $b=\tau a_0$, with $\tau \geqslant 1$ a finite number, and $c_0=\frac{1}{h} \gg 1$:

$$\Gamma\left(a_0,\tau a_0,\frac{1}{h}\right) = -\frac{(\tau-1)a_0}{2[1+a_0(1+\tau)]} + O(h)$$

and

$$\Lambda\left[a_0,\tau a_0,\frac{1}{h}\right] = \frac{h}{2} + O(h^2).$$

Upon increasing τ away from 1, (Γ,Λ) approaches the segment

$$\left[-\frac{(\tau-1)a_0}{2[1+a_0(1+\tau)]},0\right]$$

of the negative γ axis. Actually, the whole segment $(-1/2,0]$ can be approximated since for $b \gg 1$, but $b=o(1/h)$, (Γ,Λ) approaches the point $(-1/2,0)$. To see this, we set $b=1/\sqrt{h}$ and $c=1/h$, so that

$$\Gamma\left[a_0,\frac{1}{\sqrt{h}},\frac{1}{h}\right] = -\frac{1}{2} + O(\sqrt{h}) \text{ and } \Lambda\left[a_0,\frac{1}{\sqrt{h}},\frac{1}{h}\right] = \frac{\sqrt{h}}{2} + O(h).$$

Finally, to reach the line segment $\lambda+2\gamma+1=0$ we set $b=\nu a_0/h$ and $c=1/h \gg 1$, with ν a finite number such that $\nu a_0 < 1$, so that

$$\Gamma\left[a_0,\frac{\nu a_0}{h},\frac{1}{h}\right] = \frac{1}{\nu a_0 - 2} + O(h),$$

$$\Lambda\left[a_0,\frac{\nu a_0}{h},\frac{1}{h}\right] = \frac{\nu a_0}{2-\nu a_0} + O(h).$$

It is interesting to heed that upon approaching the boundary of the admissible region (4.3), to leading terms the interaction strength $U_0 \propto (-k_{2,00})$ diverges as

$$k_{2,00}\left(a_0,\nu a_0,\frac{1}{h}\right) \propto (-h^{-2}), \quad k_{2,00}\left(a_0,\frac{1}{\sqrt{h}},\frac{1}{h}\right) \propto (-h^{-5/2}),$$

$$k_{2,00}\left(a_0,\frac{\nu a_0}{h},\frac{1}{h}\right) \propto (-h^{-3}).$$

APPENDIX D: STRALEY'S PLATELETS

For completeness, we derive here from Eqs. (4.9) and (3.8)–(3.10) the expressions for γ and λ corresponding to the quadrupolar projection of the excluded volume between a pair of equal Straley's platelets [8,10]:

$$\gamma = \frac{(\ell^2-b)(b-1)}{2b(1+\ell^2)+2(b^2+\ell^2)-\ell(1+b^2)-6b\ell}, \quad \text{(D1a)}$$

$$\lambda = \frac{\ell(b-1)^2}{2b(1+\ell^2)+2(b^2+\ell^2)-\ell(1+b^2)-6b\ell}, \quad \text{(D1b)}$$

where, as in [12], b and ℓ denote the platelet's breadth B and length L scaled to the platelets' width W. As for all spherocuboids, the values attained by γ and λ in Eqs. (D1) for all possible choices of the geometric parameters B, L, and W correspond to a partly repulsive quadrupolar interaction.

[1] L. Onsager, Ann. N.Y. Acad. Sci. **51**, 627 (1949).
[2] W. Maier and A. Saupe, Z. Naturforsch. **13a**, 564 (1958). [Translated into English in T. J. Sluckin, D. Dunmur, and H. Stegemeyer, *Crystals that Flow* (Taylor and Francis, London, 2004), pp. 381–385].
[3] A. M. Somoza and P. Tarazona, J. Chem. Phys. **91**, 517 (1989).
[4] A. M. Somoza and P. Tarazona, Mol. Phys. **75**, 17 (1992).
[5] S. Romano, Int. J. Mod. Phys. B **9**, 85 (1995).
[6] P. Tarazona, Philos. Trans. R. Soc. London, Ser. A **344**, 307 (1993).
[7] J. D. Weeks, D. Chandler, and H. C. Andersen, J. Chem. Phys. **54**, 5237 (1971).
[8] J. P. Straley, Phys. Rev. A **10**, 1881 (1974).
[9] N. Boccara, R. Mejdani, and L. De Seze, J. Phys. (France) **38**, 149 (1977).
[10] B. Mulder, Phys. Rev. A **39**, 360 (1989).
[11] A. M. Sonnet, E. G. Virga, and G. E. Durand, Phys. Rev. E **67**, 061701 (2003).
[12] F. Bisi, E. G. Virga, E. C. Gartland, Jr., G. De Matteis, A. M. Sonnet, and G. E. Durand, Phys. Rev. E **73**, 051709 (2006).
[13] G. S. Singh and B. Kumar, Ann. Phys. (N.Y.) **294**, 24 (2001).
[14] A. Isihara, J. Chem. Phys. **18**, 1446 (1950).
[15] B. Tjipto-Margo and G. T. Evans, J. Chem. Phys. **94**, 4546 (1991).
[16] R. Schneider, *Convex Bodies: The Brunn-Minkowski Theory*, Encyclopedia of Mathematics and its Applications Vol. 44 (Cambridge University Press, Cambridge, U.K. 1993).
[17] B. Mulder, Liq. Cryst. **1**, 539 (1986).
[18] M. P. Taylor, Liq. Cryst. **9**, 141 (1991).
[19] B. M. Mulder, Mol. Phys. **103**, 1411 (2005).
[20] M. A. Cotter, in *The Molecular Physics of Liquid Crystals*,

edited by G. R. Luckhurst, and G. W. Gray (Academic Press, London, 1979), Chapt. 7.
[21] M. Fiałkowski, A. Kapanowski, and K. Sokalski, Mol. Cryst. Liq. Cryst. Sci. Technol., Sect. A **265**, 371 (1995).
[22] M. E. Rose, *Elementary Theory of Angular Momentum*, unabridged, unaltered republication of the work originally published by Wiley, New York, 1957 (Dover, New York, 1995).
[23] R. F. Kayser, Jr. and H. J. Raveché, Phys. Rev. A **17**, 2067 (1978).
[24] H. Goldstein, *Classical Mechanics*, 2nd ed. (Addison-Wesley, Reading, MA, 1980).
[25] G. De Matteis, S. Romano, and E. G. Virga, Phys. Rev. E **72**, 041706 (2005).
[26] M. J. Freiser, Phys. Rev. Lett. **24**, 1041 (1970).
[27] M. J. Freiser, Mol. Cryst. Liq. Cryst. **14**, 165 (1971).
[28] L. Longa, P. Grzybowski, S. Romano, and E. G. Virga, Phys. Rev. E **71**, 051714 (2005).
[29] G. De Matteis, F. Bisi, and E. G. Virga (unpublished).
[30] R. Blaak, B. M. Mulder, and D. Frenkel, J. Chem. Phys. **120**, 5486 (2004).
[31] K. Merkel, A. Kocot, J. K. Vij, R. Korlacki, G. H. Mehl, and T. Meyer, Phys. Rev. Lett. **93**, 237801 (2004).
[32] G. De Matteis, and E. G. Virga, Phys. Rev. E **71**, 061703 (2005).
[33] D. M. Brink and G. R. Satchler, *Angular Momentum* (Oxford University Press, Oxford, 1962).